Journal of Control, Automation and Electrical Systems (2020) 31:73–83
https://doi.org/10.1007/s40313-019-00514-6

Development of an Online Automated Fabric Inspection System

Saulo Vargas[1] · Maurício Edgar Stivanello[2] · Mário Lúcio Roloff[3] · Éderson Stiegelmaier[1] · Marcelo Ricardo Stemmer[4]

Received: 18 March 2019 / Revised: 14 August 2019 / Accepted: 21 August 2019 / Published online: 28 August 2019

Abstract
In this work, the development of a system for the automated inspection of mesh fabrics in real time through computer vision techniques is described. Here, a processing pipeline that includes a distortion removal procedure, a texture-based detector, a shape and an artificial neural network classifier is proposed. Different from other works found in the literature, the developed system was evaluated under real inspection conditions. The obtained results show that the proposed system not only achieves compatible defect detection and classification rates than the current state-of-the-art methods but also met functional and non-functional requirements observed in industry.

Keywords Automatic optical inspection · Knitted fabric · Machine vision · Quality control · Textile industry

1 Introduction

Quality control at all stages of the textile production chain is an important business strategy for companies in this segment, enabling them to compete on the global market. The current scenario calls for increased production efficiency, with more agile production lines, reduced waste creation and better final product quality.

Specifically, in the fabric production stage, the preliminary inspection allows feedback in the production process, preventing the reoccurrence of defects with known cause. Therefore, it is possible to increase the yield of subsequent steps, avoiding reprocessing and reducing the generation of textile waste. Fabrics with faults or defects account for approximately 85% of the defects found in the clothing industry (Sengottuvelan et al. 2008). Thus, the pre-inspection of the fabric is an important phase of the quality control.

Most of the nonconformities in fabrics in the production stage are still identified by human operators. The inspection is performed with the aid of rewinding machines which unwind the fabric at a constant speed of 8 to 20 m/min on a table illuminated by a backlight (Kumar 2008). However, considering the time required and level of precision, these manual inspections are not appropriate for satisfying the highly competitive demands of the global market (Habib et al. 2014). The accuracy of manual inspection is estimated to be around 70%, and it is strongly influenced by human operator fatigue (Li and Zhang 2016; Ngan et al. 2011; Islam et al. 2008).

Due to the importance of prior inspection of the fabric to ensure the quality of the final product, several researchers are carrying out studies aimed at proposing systems or techniques for the automated inspection of fabric based on machine vision (Li and Zhang 2016; Li et al. 2013; Zhou et al. 2016; Kumar 2008; Ngan et al. 2011; Mahajan et al. 2009). However, although advances have been achieved in this area of research, few papers have addressed the challenges observed under real inspection conditions at industrial plants, such as the high speed at which the fabric moves and real-time constraints.

In this work, the development of an automated system for online fabric inspection based on computer vision is described. The main contributions of this paper are as follows:

1. The proposal of a multistep inspection method for defects detection and classification. In this method, a calibration step is used, allowing the location of defects in metric units. The segmentation and description of tissue defects

✉ Saulo Vargas
saulo.vargas@ifsc.edu.br

1 Federal Institute of Santa Catarina, Gaspar, Brazil
2 Federal Institute of Santa Catarina, Florianópolis, Brazil
3 Catarinense Federal Institute, Rio do sul, Brazil
4 Federal University of Santa Catarina, Florianópolis, Brazil

are done based on statistical descriptors, and the classification is done based on morphological or texture analysis.
2. The evaluation of results under real inspection conditions for both detection and classification steps.
3. The creation of an image dataset for fabric defects acquired directly from a tissue rewinder and classified by a specialist. This dataset was made available on the Web.

The approaches used in automated fabric inspection in the literature are described in Sect. 2. Section 3 details the approach used in the development of the proposed system, including the proposal of defect detection and classification methods and a general description of the inspection system. In Sect. 4, the experimental results obtained in the evaluation of the system using images of the surface of the fabric taken in real time are discussed. Finally, in Sect. 5 the conclusions and perspectives for future work are presented.

2 Automated Fabric Inspection: A Review

The methods used in automated fabric inspection systems described in the literature vary according to the characteristics of the fabric and are classified according to the approach used to analyze the texture (Kumar 2008; Ngan et al. 2011; Mahajan et al. 2009). The adopted approaches are commonly classified into three categories: *statistical*, *spectral* and *model based*.

Considering that regions of non-defective fabric are somehow stationary, statistical approaches detect defects as being the regions with statistically different behavior. The spatial distribution of intensity levels in this approach is defined by representations such as co-occurrence matrices, fractal dimension, cross-correlation and mathematical morphology.

Images of fabric with uniform texture, composed of standardized repetitions of texture primitives, are more easily evaluated in the frequency domain. In this spectral approach, primitive texture features can be described using Fourier transform, Gabor filter or wavelet transform techniques. The occurrence of spectral changes can then be interpreted as the presence of a defect in the region of the fabric being inspected.

Model-based approaches are particularly suited to images of random-textured fabric. In this case, the textures are modeled by stochastic processes using, for instance, autoregressive models or Markov random fields. Thus, the detection of defects corresponds to the problem of testing the statistical hypothesis of the model.

According to the taxonomy of methods for the automated detection of fabric defects organized by Ngan et al. (Ngan et al. 2011), the hit rates range from 54.13 to 98.30% for the statistical approach methods and from 82.86 to 98% for the spectral approach methods, with values up to 100% for the methods that fall within the model-based approach.

In addition to detection, classification of the defect according to its nature or categories of defects, instead of binary classification (whether or not defective), is a primary task in fabric quality control. This information can be used to prevent the recurrence of defects from known causes and can be applied to classify the fabric roll based on its quality grade. For the automated execution of this task, neural network classifiers (Habib et al. 2014), fuzzy logic (Kumar and Ragupathy 2012) and support vector machines (Dongli et al. 2013) are used. Most approaches are based on neural networks, according to Habib et al. (2014).

The selection of the descriptors used in the characteristic vectors that represent the different types or categories of defects has a great influence on the performance of the classifier (Gonzalez and Woods 2008). Different descriptors have been used as inputs for classifiers of fabric defects. Geometric descriptors, such as the centroid, height, width and area of the defective region, and histogram-based texture descriptors, such as homogeneity, entropy and contrast, based on co-occurrence matrices, are examples of descriptors used as components of the feature vector.

Several types of defects can arise in fabric production. However, the type of artifact generated by certain groups of defects in images of defective regions has led researchers to define categories of defects (Stivanello et al. 2016). The categories of defined defects include: hole, oil stain, yarn color, missing vertical thread, missing horizontal thread and other type of defect. In addition, there is the category without defects, defined in systems that do not perform a previous stage of defect detection and where the classifier evaluates all inspected images.

The criterion most commonly used to evaluate the performance of the classifiers is the overall classification accuracy, which corresponds to the probability that any image (or defect) is correctly classified among the output categories. According to the comparative study of classifiers based on neural networks, organized by Habib et al. (2014), the values for the overall precision of these classifiers range from 76.5 to 100%. The global accuracy for the fuzzy-based classifier was 96.55%, and for the SVM-based classifier it was 94% (Dongli et al. 2013).

Despite the extensive literature available on the subject, it is important to note that the existing methods are often evaluated under operating conditions which are very different from those found in industrial practice. It is common, for example, to use a small number of samples or images acquired from static fabric (Kumar 2008; Habib et al. 2014; Ngan et al. 2011; Mahajan et al. 2009). The few works that evaluate the automated inspection considering real-time issues are limited to the task of defect detection (Zhou et al. 2016; Li et al. 2013).

3 Description of the Proposed Automated Fabric Inspection System

Observing the application domain, we have that the main functional requirements to be met by the automated inspection system are:

- Detection and classification of the defects present in rolls of mesh fabric according to the categorization of defects employed by industry;
- Calculation of the number of defects and the total defective area in each inspected roll.

Moreover, the most important non-functional requirements to be observed are:

- The accuracy must be equal to or greater than that achieved in manual inspection: 70% (Ngan et al. 2011; Islam et al. 2008);
- The inspection speed must be compatible with the operating conditions found in the industry: up to 20 m/min (Kumar 2008).

The details of the automated image-based inspection system proposed to meet these requirements are followed in sequence.

3.1 Inspection System Architecture

In Fig. 1, a simplified architecture of the proposed system is shown. Here, the inspection is performed from images of the surface of the fabric, obtained from an acquisition and processing system coupled to a reviewing machine, similar to those used in the textile industry for manual inspection.

An incremental encoder is installed in the reviewing machine to control the speed and synchronize the images acquisition and inspection. It is also used to calculate the length of inspected roll. A camera is used to capture images from the surface of the fabric. In turn, a computer is used to process each of the images and record the inspection information of the roll.

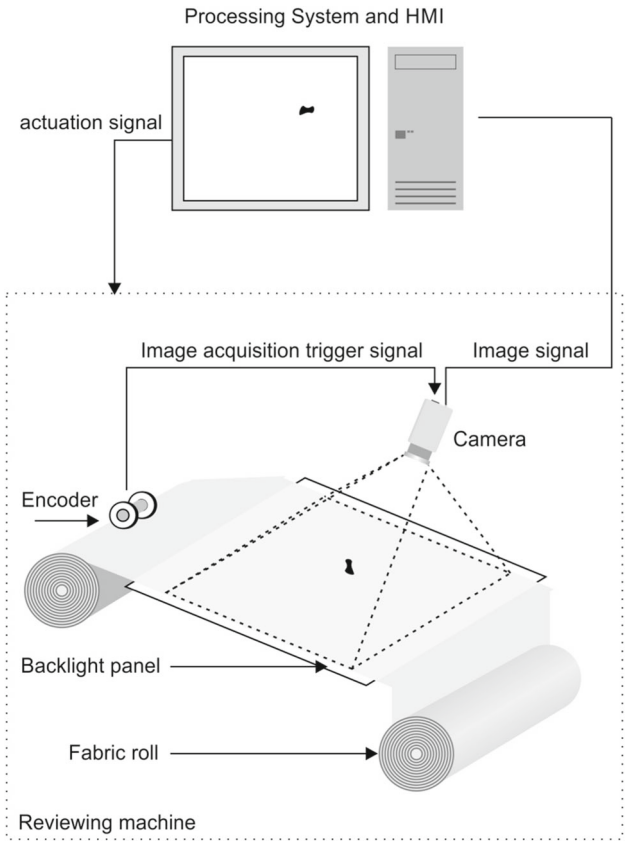

Fig. 1 Simplified architecture of the proposed system

3.2 Detection and Classification of Defects Through Computer Vision Techniques

The presence of defects in a fabric surface sample causes visual changes that can be described through an analysis of the intensity levels of the image. Therefore, a statistical approach was used for the automated inspection of defects. Figure 2 shows a flowchart of the adopted processing pipeline.

Initially, a configuration step is performed to obtain calibration parameters used in the correction of images and in the conversion of measurements necessary to calculate the defective area information and length of the fabric roll. During the inspection, an image of each region of the fabric surface is acquired. Each image is preprocessed in an *Image correction* step in order to remove projective distortions. Then, the image is processed in a *Defect detection* step to verify if it reveals any defective region. If the result is positive, these regions are processed in a *Texture descriptors calculation* step. Texture descriptors are used in a *Defect classification* step to determine which category the region fits. A report containing information relevant to the industrial process, such as the defective area and amount of defects per fabric roll, is generated, based on the records of detection and classification of defects of the roll.

The main steps of the described pipeline are followed in sequence.

3.2.1 Camera Calibration and Image correction

Imperfections in the optical system cause distortions in the geometric characteristics of the captured image. Light rays farther from the center of lens are bent too much compared to rays that pass closer to the center. Thus, straight lines can appear to bow out on the image plane. Some of the defects to

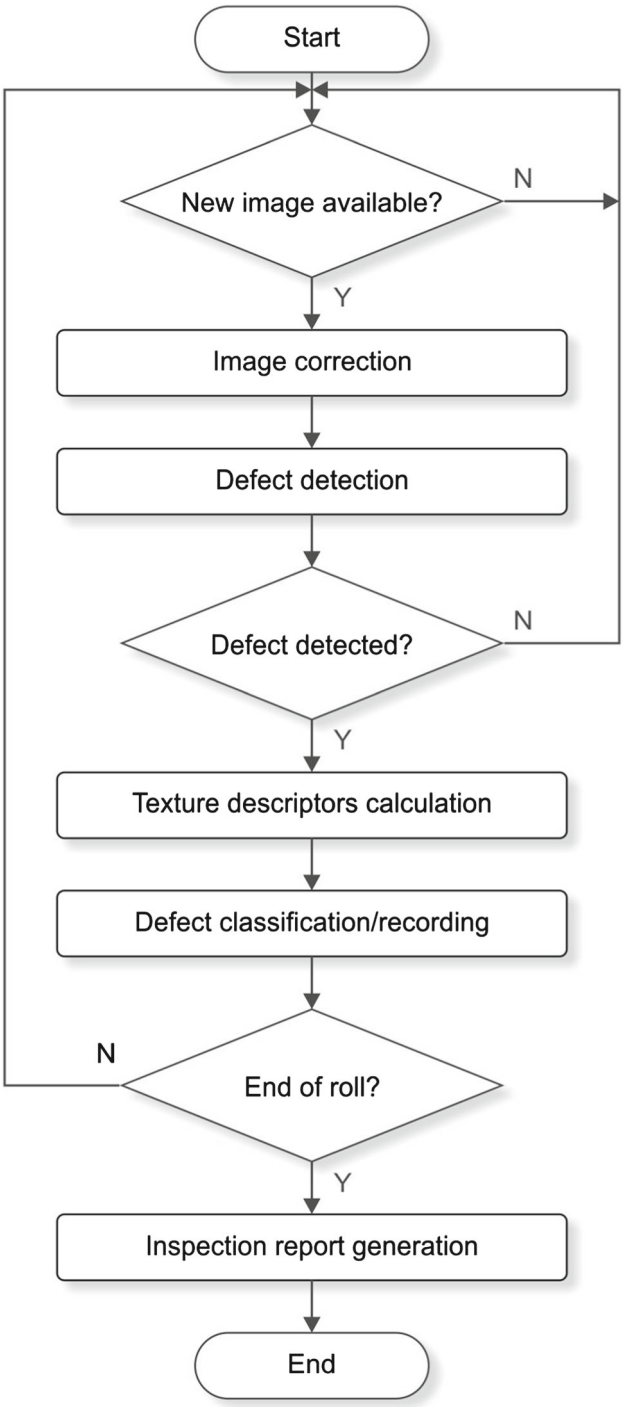

Fig. 2 Flowchart of the processing steps

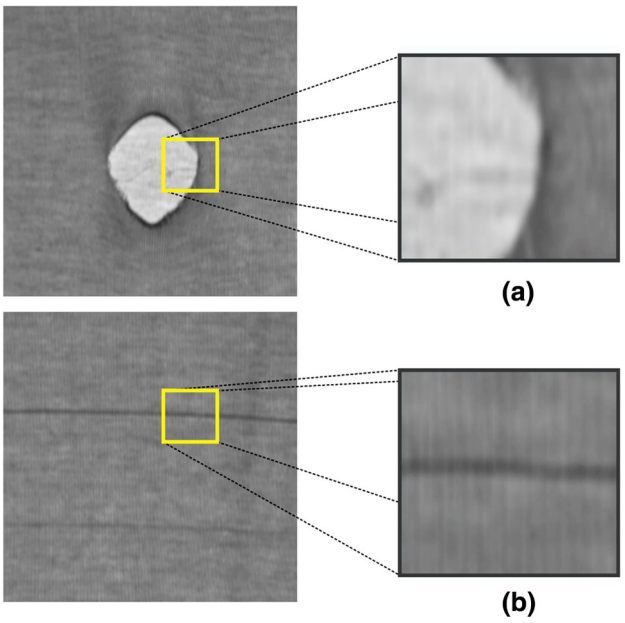

Fig. 3 Subwindows located in defective regions

be detected and classified in the proposed system are characterized by vertical and horizontal straight lines. Thus, such distortions must be removed, considering that the detectors employed to detect lines only work on undistorted images.

In order to estimate the radial coefficients and the perspective transformation that describes such distortions, a camera calibration method is applied (Zhang 2000). The perspective transformation matrix and the distortion coefficients can be used to compute the joint undistortion and rectification transformation in the form of maps or lookup tables (LUT). These maps can be used to recover the original geometric characteristics of the fabric image.

In turn, in order to obtain information such as the position and length of the detected defect, it is necessary to convert the coordinates in pixels in the plane of the image to metric coordinates, according to a coordinate system of the plane of the observed fabric. The conversion of coordinates between the systems involved is performed through the estimation of projective transformation, or homography, which relates the two planes (Trucco and Verri 2003).

3.2.2 Defect Detection

For the detection of defects, a method based on local statistics is applied (Stivanello et al. 2016). The method consists of dividing the image to be inspected into small square regions or subwindows and evaluating the texture in each one of them. This method is based on the premise that the pixels around the border of defective regions have very different levels of intensity. In fabric images where there are defects that result in *greater passage of light* in the defective region, such as holes and tears, the subwindow contains pixels with levels of intensity close to the ends of the gray scale, in addition to pixels with the same intensity levels as the regions without defects, as shown in Fig. 3a. In cases where the defects are not evidenced by the "greater passage of light" because they are more closed, as is the case of Fig. 3b, the subwindow contains

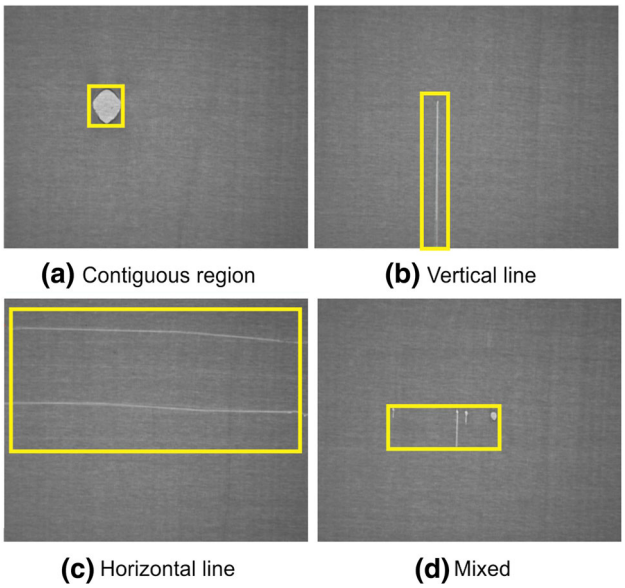

Fig. 4 Defective region identification

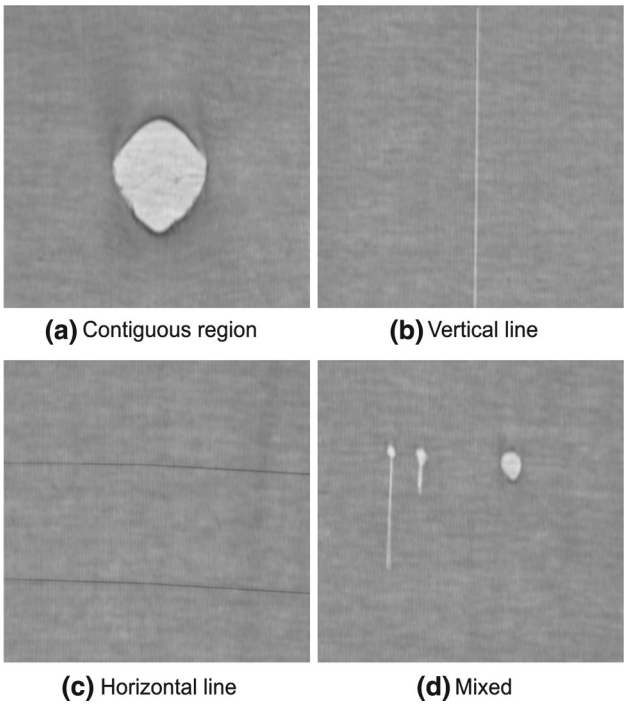

Fig. 5 Categories of defects

pixels with intensity levels that vary from the darkest level to the levels present in regions without defects.

It is possible to observe that the texture in the areas surrounding the border of defective regions is not very smooth, indicating a high variability of the intensity levels. In regions without defects, the opposite is observed, that is there is less variability and the texture is smoother. Based on these observations, to describe the texture of the subwindows of the image a softness descriptor standard deviation is used. This is calculated employing the second statistical moment of the intensity histogram of each subwindow. The limit value for the standard deviation which indicates the presence of a defect is automatically determined for each type of mesh and subwindow size from the mean value of the subwindow standard deviations of a user-defined non-defective image range.

3.2.3 Texture Descriptor Calculation

As shown in Fig. 4, the defective regions have different textures for each defect category. The region bounded by the smallest rectangle that circumscribes all defects of a captured image was defined as a defective region.

The combinations of the different intensity levels of each defective region are mapped on a co-occurrence matrix, allowing the description of the texture through statistical gray-level occurrences, such as contrast, uniformity, homogeneity, entropy and correlation (Gonzalez and Woods 2008).

3.2.4 Defect Classification

The automated classification of visible defects is not a simple task as some groups of defects produce similar artifacts in fabric images of defective regions. This fact, coupled with the absence in the literature of a categorization of fabric defects that considers the topological characteristics of the defect, led us to use a previously defined simplified and comprehensive categorization built together with professionals of the textile industry (Stivanello et al. 2016).

Due to the similarity of the artifacts generated by certain groups of defects observable in defective region images, four categories of defects were defined, *contiguous region (CR)*, *vertical lines (VL)*, *horizontal lines (HL)* and *mixed*. These categories encompass the most relevant defects observed in the industry according to experts, and the proposed categorization has enough granularity to aid in diagnostics based on the history of occurrence of the defects. The defect categories were designed in such a way to be mutually exclusive, that is, no defect can be classified in more than one category. In addition, each defect must be classified in one of the proposed categories.

Figure 5 shows samples of the four defect categories. The category *Contiguous region* is associated with defects such as *holes* and *dye marks* or *spots*. As shown in Fig. 5 a, it is characterized by artifacts formed by clusters of pixels in the shape of spot or blob with intensities different from that of the background of the image. The categories *Vertical lines* and *Horizontal lines*, shown in Fig. 5b, c, are associated with defects such as *ladder*, *missing Plush Loop*, *spirality*, *wrong end*, *among others*. These categories are characterized by artifacts in the form of vertical or horizontal lines, respec-

tively. In turn, in Fig. 5d is shown the category *Mixed* that differs from the others because it contains more than one type of artifact in the same image.

For the automated classification of the defects detected, two methods of classification are selected: one based on *the morphological analysis of the artifacts shapes* and the other based on *the texture analysis using an artificial neural network*.

In the method based on the shape of the artifact, the classification is performed as a function of the characteristics of the shape of the artifact observed on the inspected image, as described in (Stivanello et al. 2016). To identify and describe the artifacts, image processing techniques, such as thresholding and labeling of connected components for contiguous regions and edge detectors and the Hough transform for lines, are used (Gonzalez and Woods 2008; Molina et al. 2013). The identified contiguous region artifacts will be classified as *Contiguous Region* defects. For the artifacts identified as lines, the classification will be based on the length of each segment and its angulation, those with a value outside the acceptable range being disregarded. Linear artifacts with an angle of around 90° are classified as *Vertical Line* defects and with an angulation around 0° as *Horizontal Line* defects. Classification in the *Mixed* defect category occurs when at least two of the three previous artifacts are identified in the same image, or none of these artifacts is identified.

In the second method of classification, the texture descriptors based on the co-occurrence matrix of the defective region, described in Sect. 3.2.3, are used as input for a multilayer perceptron artificial neural network (MLP) (Gonzalez and Woods 2008; Haykin 1998; Moreira et al. 2018). In Fig. 6, a simplified architecture of the proposed MLP defects classifier is shown.

For each defective image, four co-occurrence matrices of the defective region were obtained, with a distance between pixels of 1 pixel and orientations of 0°, 45°, 90° and 135°. For each matrix, we calculated the descriptors of the texture, such as the contrast, uniformity, homogeneity, entropy and correlation, as described in (Gonzalez and Woods 2008), resulting in 20 descriptors. An input layer and a hidden layer with 20 neurons each and a four-neuron output layer are used, representing each category of defect. A sigmoid function is used for neurons activation function, and the supervised learning based on back-propagation is used for training.

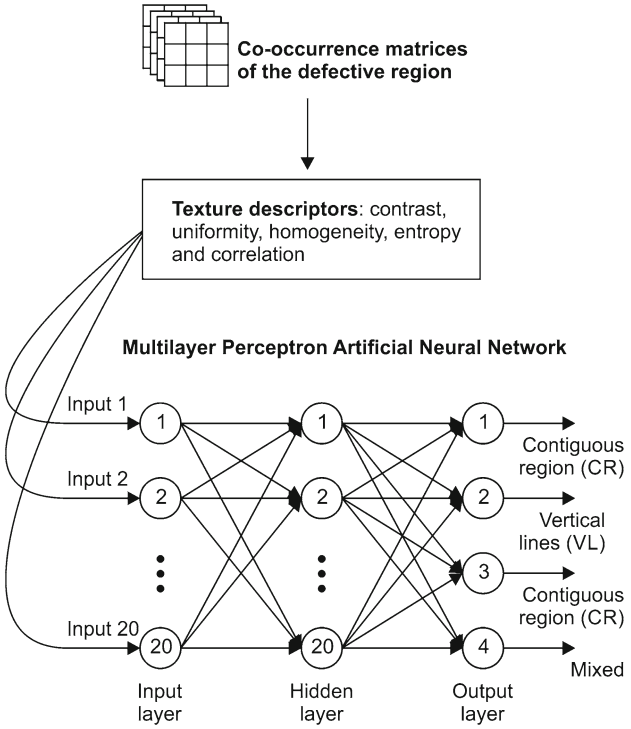

Fig. 6 MLP-based defects classifier architecture

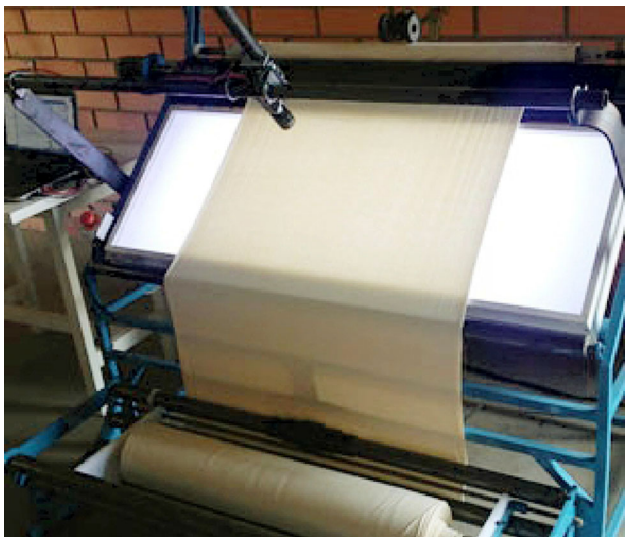

Fig. 7 Inspection machine

4 Experimental Results

4.1 Developed System

The machine implementing the system described in Sect. 3 is shown in Fig. 7. The specifications of the components used in the acquisition and processing are given in Table 1. The software of the system was implemented in C++.

The system must be calibrated at a preliminary stage prior to use in tissue inspection. Table 2 shows the distortion coefficients k1, k2, k3, k4 and k5 estimated for the described optical system in the calibration process by using a planar pattern (Bradski and Kaehler 2013; Drap and Lefèvre 2016). Such coefficients are used in the rectification of the images so that the distortions caused by imperfections of the optical system

Table 1 Components specifications

Component	Characteristics
Camera	acA1300-60gm, Sensor: CMOS, Res.: 1282 x 1026 pixels, Interface: GigE
Lens	TAMRON 12VM412ASIR, Focal dist.: 4-12 mm, Sensor size: 1/2" Manual iris
Encoder	AUTONICS ENC-1-2-T-24, Res. 1 cm/pulse, Max. speed: 5000 rpm, 100 pulses per revolution
Computer	DELL Latitude 3440, Processor: INTEL Core i7-4500U 1.80 GHz, RAM: 8GB

Table 2 Radial distortion coefficients

Coefficients	Estimated value
k1	-4.035×10^{-1}
k2	4.453×10^{-1}
k3	-5.604×10^{-3}
k4	-2.428×10^{-3}
k5	-1.102×10^{0}

are removed, as described in Sect. 3.2. Recent works have demonstrated the numerical effectiveness of the correction of optical distortions by means of such digital technique Gao et al. (2017). Its application in the present work was shown to be effective due to the accuracy achieved in the detection of straight lines, as discussed in the following sections.

4.2 Creation and Usage of an Image Dataset for Fabric Defects

The evaluation of the proposed inspection system was performed based on the image acquisition and processing system described in Sect. 4.1. A roll of raw knitted fabric, produced with a 24/1 Ne thread on an industrial loom, with a length of 23.30 m and a width of 0.90 m, was used for the evaluation of the system. The camera was adjusted at a working distance of 35 cm from the plane of the fabric, which resulted in a field of view of 0.40 m width by 0.30 cm height.

Images were captured from this roll of mesh fabric being unwound in the prototype of rewinding machine at a roll speed of 20 m/min, reproducing the operating conditions found in the industry. In order to obtain a ground truth, each image obtained by the system was manually inspected in detail by a textile specialist to create a reference for comparison with the automated inspection result. Seventy-five samples of fabric surface were available, of which 48 are defect-free regions and 27 contain some artifacts corresponding to a defect generated by some type of defect.

The manual inspection report for one face of the fabric roll used is shown in Table 3. The area of each defect was calculated by multiplying the defect length by the width considered of the inspected fabric (0.40 m).

Table 3 Manual inspection report

Characteristics	Value
Length	23.30 m
Width	0.40 m
Inspected area	9.32 mm^2
Number of defects	17
Defective area	1.46 m^2
Defective area percentage	15.66%

Table 4 Defects found in the manual inspection

Defect Category	Quantity
Contiguous region	7
Horizontal line	3
Vertical line	4
Mixed	3

Table 5 Detection report

Subwindow	Hits (%)	Misses (%)	False positives (%)	False negatives (%)
8 × 8	93.33	6.67	0	18.52

Table 4 shows the types of defects present in the inspected fabric roll, as categorized in Sect. 3.2.4, as well as the respective quantities.

In order to support future works in automatic fabric inspection, the described image dataset is freely available to the scientific community [1]

4.3 Detection Results

Table 5 shows the real-time defect detection results obtained with the system when using subwindows of size 8. It is known that large subwindows do not circumscribe small defect boundaries, but rather the whole defect. Also, that small subwindows consume more processing time (Stivanello et al. 2016). Hence, the chosen size was determined empirically to give a trade-off between improved accuracy and processing speed and was set to cover the entire area of the inspected image. For the 48 frames without defects, the system did not generate false positives, that is, no frame without defects was falsely classified as defective. For the 27 frames with defects, the system generated 5 false negatives, that is, 5 frames with defects were falsely classified as being without defects.

The detection method used showed a higher precision than traditional manual inspection, which is approximately 70%

[1] Knitted Fabric Dataset: http://fabricdataset.gaspar.ifsc.edu.br.

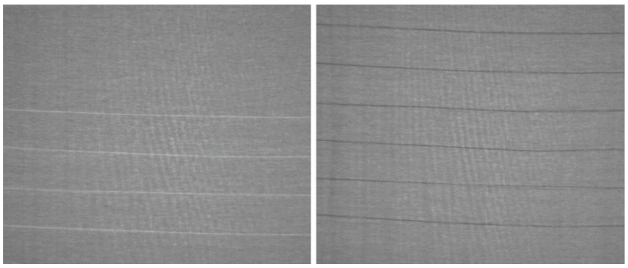

Fig. 8 Examples of horizontal line-type defects

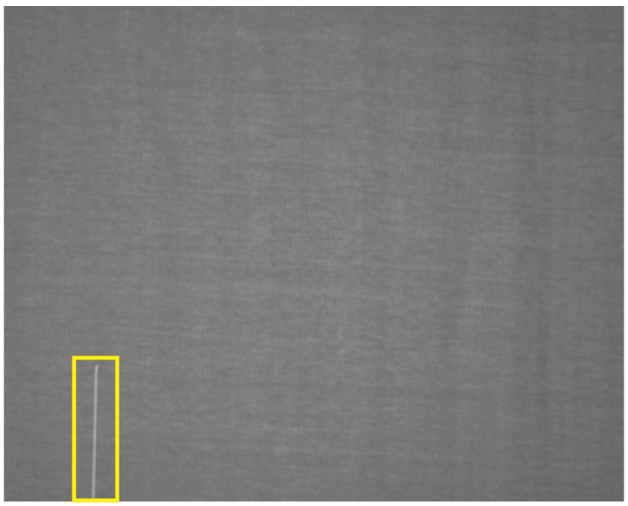

Fig. 9 Examples of vertical line-type defects

(Ngan et al. 2011; Islam et al. 2008). This result is consistent with the results for detection systems reported in the literature, according to the taxonomy of methods for the automated detection of fabric defects organized by (Ngan et al. 2011), and with the results presented in (Stivanello et al. 2016), in which the same detection approach was used, but where the evaluation was not carried out in real time.

The 22 true positive frames detected by the inspection system correspond to 15 defects of those detected by the specialist. This is due to the fact that some defects were captured by more than one frame due to its size. The 2 defects not detected by the method correspond to defects of the horizontal line type.

The proposed detection method did not prove to be robust in the detection of horizontal line-type defects, as illustrated in Fig. 8. In cases where this type of defect was detected, the detected region corresponds to a small part of the defect.

All defects of the vertical line-type were detected by the proposed method, but for some images of this type of defect, as shown in Fig. 9, the defect was also not completely detected. Due to the texture of the inspected mesh fabric, the image intensities of some horizontal and vertical line-type defects are similar to the intensities of non-defect regions.

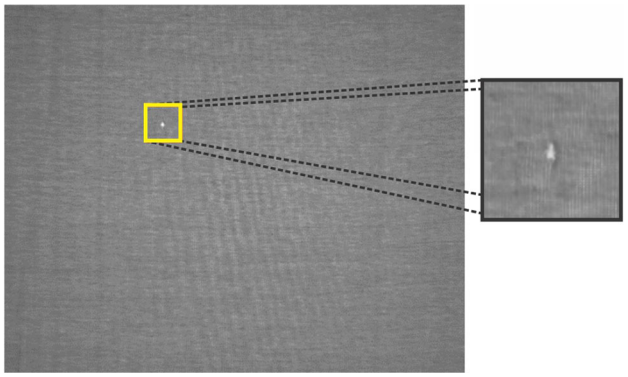

Fig. 10 Example of contiguous region-type defect

This is due to the grammage of the yarn, which originated a thinner fabric with a more open weave.

A reduction or increase in the subwindow size did not influence the efficiency of the detection method for these two types of defects. In addition to not contributing to the detection, the reduction slows down the system. Increasing the size of the subwindows reduces the number of subwindows with a standard deviation greater than the threshold and impairs the detection of small defects.

If the threshold value is reduced to detect these two defects, the number of subwindows that result in false positives will be increased due to the fabric texture and this will impair the performance of the detection method.

For defects that generate in the inspected image, an artifact with gray levels which differ from the background of the image, the method detected all defects present in the roll used, the smallest defect being 5 mm long by 3 mm wide, as shown in Fig. 10.

4.4 Results for the Calculation of Defective Area and Defect Marking

To meet the requirement to calculate the total defective area, the distance between the lines limiting the detected defect was used to determine the individual defective length, as shown in Fig. 11.

Considering only true positive frames, the total defective length determined by the inspection system was 1.64 m, which results in a total defective area of 0.66 m^2 (1.64 × 0.4). On comparing this value with the total area of the 15 corresponding defects detected by the specialist (1.38 m^2), we find that the system calculated only 48% of the defective area generated by these defects.

If horizontal and vertical line defects are disregarded, since the system did not detect all of these defects completely, it is observed that the defective area detected by the system is 94% of the defective area detected by the specialist. This

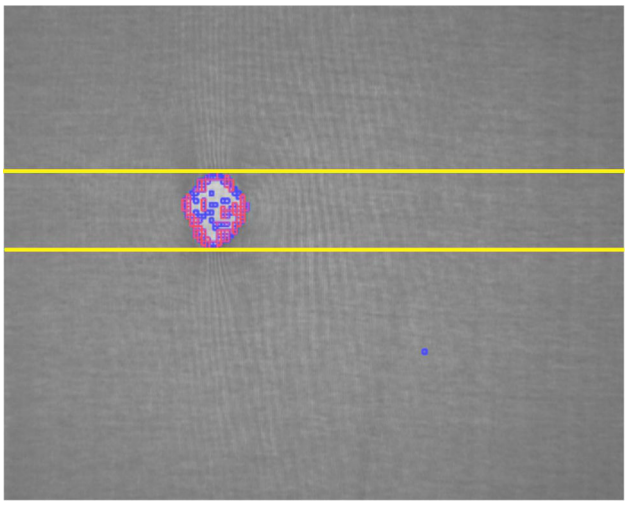

Fig. 11 Calculating the length of the defect

Table 6 Confusion matrix—shape-based method

Category	HL	VL	CR	Mixed	Precision (%)
HL	2	0	0	0	100
VL	0	8	0	1	89
CR	0	0	6	1	86
Mixed	0	0	1	3	75

number did not approach 100% because a mixed-type defect has a vertical line that was not completely detected.

To highlight the defect with some type of marking, the system returns the coordinates of the defect boundaries in the margin of the plane of the fabric, from the position of the lines that delimit it in the plane of the image. These coordinates can be used by an actuator to make markings located at the edge of the fabric roll, similar to the procedure followed by a human inspector.

4.5 Classification Results

The results obtained by the shape-based and RNA-based classification methods were compared with the classification made by the specialist from the textile industry. These results were organized through a confusion matrix, from which the accuracy by category, overall precision and Kappa coefficient are calculated.

Tables 6 and 7 present the confusion matrix with the accuracy of the classifiers by category in the last column. The overall precision and Kappa coefficient are shown in Table 8.

The shape-based method presented good accuracy rates within each category. The mixed defect, wrongly classified as a contiguous region, is formed by a contiguous region and a horizontal line. The error occurred because

Table 7 Confusion matrix—RNA

Category	HL	VL	CR	Mixed	Precision (%)
HL	2	0	0	0	100
VL	1	7	1	0	78
CR	0	0	7	0	100
Mixed	1	0	1	2	50

Table 8 Global precision and Kappa coefficient

	Shape-based method (%)	RNA-based method (%)
Global precision	86	82
Kappa coefficient	80	74

the artifact generated by the line was not identified by the proposed method. The vertical line and contiguous region defects, erroneously classified as mixed, were generated in the captured images artifacts with intensities close to the bottom of the image and therefore were not identified, causing the system to classify them as mixed. A refinement of the method parameters used to identify these artifacts would reduce the efficiency of the shape-based classification method.

The method based on RNA presented good accuracy rates for the categories horizontal line, vertical line and contiguous region, but the method was not efficient in the classification for the mixed category.

Classification methods evaluated in real time presented similar overall accuracy rates, with a small advantage for the form-based method. Based on these rates, it can be stated that the probability of the correct classification of these methods for a new image is around 80%.

When comparing the results for these classification methods with those found in the literature, it can be observed that the global accuracy rates were within the precision range of studies based on neural networks (76.5% to 100%) (Habib et al. 2014). However, they were slightly below the results of methods based on fuzzy logic (96.55%) (Kumar and Ragupathy 2012), SVM (94%) (Dongli et al. 2013) and form-based techniques (100%) (Stivanello et al. 2016).

Considering the results for the inspection system, the proposed detection and classification approaches prove to be satisfactory, with the advantage that the evaluation was carried out in real time and in an inspection scenario similar to that in an industrial textile plant. In addition, if we consider that manual inspection reaches rates estimated at about 70%, we can consider that the use of the proposed system is advantageous.

Table 9 Average processing times (ms)

Method	Detection	Classification	Total
Detector + RNA classifier	0.13	0.08	0.21
Detector + Shape classifier	0.13	0.06	0.19

4.6 Computing Time

The computer described in Table 1 was used to measure the computing time. No SIMD (single instruction, multiple data) technology was used for this execution, which ran on a single-thread process without GPU support. Images from the created dataset were used for the quantitative analysis of the results.

Table 9 shows the processing times obtained with inspection pipelines employing the defect detector combined with the shape-based and the RNA-based classifiers.

It is important to evaluate the frequency of the inspection task cycle facing the problem scope. Considering the use of a camera configuration in which the field of view is 30 cm in the longitudinal direction of the fabric roll being inspected, acting on a inspection machine at a speed of 8 to 20 m/min, which is the same range of speed applied in a traditional inspection system (Kumar 2008), it is possible to define a constraint that determines that the frequency of a complete inspection cycle should be at least 0.91 Hz. Thus, the frequencies obtained with both pipelines meet the application requirement of inspection speed by exceeding the frequency reached with the manual inspection, even without possible optimizations.

5 Conclusions and Future Work

In this paper, the development of a system for the automated inspection of plain raw mesh is described. Different computer vision techniques were combined to achieve defect detection and classification.

In contrast to other studies reported in the literature, the described system was evaluated under real conditions of use, inspecting in real-time images of the surface of the mesh fabric captured from a roll of fabric being unwound by a reviewing machine used in the textile industry. The detection rate was 93.33% for subwindows of size 8x8, and the overall accuracy rate of the classification was 86% for the shape-based method and 82% for the method based on artificial neural networks.

Despite the occurrence of detection failures, the success rates obtained are higher than those achieved by human inspectors and the classification rate is consistent with the results found in the literature. The detection of defects that form a line-type artifact in the image proved to be the greatest challenge. The adoption of the statistical-based detection method was not robust enough to detect all occurrences of this type of defect, especially for horizontal lines. However, the method proved to be robust in detecting defects which form on the image an artifact of the contiguous region type, due to the contrast between this type of defect and the rest of the image.

The type of mesh used in the evaluation of the system was found to be an important variable in relation to the efficiency of an automated vision inspection system. The weight of the yarn used in the production of the mesh fabric influences the texture of the fabric produced and, consequently, the texture of the captured images. Thus, the parameters of the detection and classification methods must be defined according to the type of fabric.

In future work, the proposed system will be evaluated using a larger base of knitted fabric rolls of the same type and for different types of raw and smooth knitted fabrics. In addition, possible optimizations by using technologies like CUDA (Compute Unified Device Architecture) or even FPGA (field-programmable gate array), for instance, will be considered in order to obtain higher inspection rates and frequencies.

Acknowledgements The authors would like to thank National Council for Scientific and Technological Development (CNPq), the University Scholarship Program of the State of Santa Catarina (UNIEDU), and the M-Galteck Co.

References

Bradski, G., & Kaehler, A. (2013). *Learning OpenCV: Computer vision in C++ with the OpenCV library* (2nd ed.). Sebastopol: O'Reilly Media Inc.

Dongli, T., Zhitao, X., Fang, Z., Lei, G., & Jun, W. (2013). Cloth defect classification method based on SVM. *International Journal of Digital Content Technology and its Applications*, *7*(3), 614–622.

Drap, P., & Lefèvre, J. (2016). An exact formula for calculating inverse radial lens distortions. *Sensors*, *16*(6), 807.

Gao, Z., Zhang, Q., Su, Y., & Wu, S. (2017). Accuracy evaluation of optical distortion calibration by digital image correlation. *Optics and Lasers in Engineering*, *98*, 143–152.

Gonzalez, R. C., & Woods, R. E. (2008). *Digital image processing*. New Jersey: Prentice Hall.

Habib, M. T., Faisal, R. H., Rokonuzzaman, M., & Ahmed, F. (2014). Automated fabric defect inspection: A survey of classifiers. *International Journal in Foundations of Computer Science & Technology*, *4*(1), 17–25.

Haykin, S. (1998). *Neural networks: A comprehensive foundation* (2nd ed.). New Jersey: Prentice Hall.

Islam, A., Akhter, S., & Mursalin, T. E. (2008). Automated textile defect recognition system using computer vision and artificial neural networks. *International Journal of Mechanical, Aerospace, Industrial, Mechatronic and Manufacturing Engineering*, *2*(1), 110–115.

Kumar, A. (2008). Computer-vision-based fabric defect detection: A survey. *IEEE Transactions on Industrial Electronics*, *55*(1), 348–363.

Kumar, K. V. N., & Ragupathy, U. S. (2012). An intelligent scheme for fault detection in textile web materials. *International Journal of Computer Applications*, *46*(10), 24–29.

Li, Y., Ai, J., & Sun, C. (2013). Online fabric defect inspection using smart visual sensors. *Sensors*, *13*(4), 4659–4673.

Li, Y., & Zhang, C. (2016). Automated vision system for fabric defect inspection using Gabor filters and PCNN. *SpringerPlus*, *5*(1), 765.

Mahajan, P. M., Kolhe, S. R., & Patil, P. M. (2009). A review of automatic fabric defect detection techniques. *Advances in Computational Research*, *1*(2), 18–29.

Molina, L., Carvalho, E. Á. N., Freire, E. O., & Freire, R. C. S. (2013). Fault-tolerant weld line detection using image processing and fusion of execution monitoring systems. *Journal of Control, Automation and Electrical Systems*, *24*(1), 70–80.

Moreira, A. C., Paredes, H. K. M., Souza, W. A., Nardelli, P. H. J., Marafão, F. P., & Silva, L. C. P. (2018). Evaluation of pattern recognition algorithms for applications on power factor compensation. *Journal of Control, Automation and Electrical Systems*, *29*(1), 75–90.

Ngan, H. Y. T., Pang, G. K. H., & Yung, N. H. C. (2011). Automated fabric defect detection—A review. *Image and Vision Computing*, *29*(7), 442–458.

Sengottuvelan, P., Wahi, A., & Shanmugam, A. (2008). Automatic fault analysis of textile fabric using imaging systems. *Research Journal of Applied Sciences*, *3*(1), 26–31.

Stivanello, M. E., Vargas, S., Roloff, M. L., & Stemmer, M. R. (2016). Automatic detection and classification of defects in knitted fabrics. *IEEE Latin America Transactions*, *14*(7), 3065–3073.

Trucco, E., & Verri, A. (2003). *Introductory techniques for 3-D computer vision*. Upper Saddle River: Prentice Hall.

Zhang, Z. A. (2000). A flexible new technique for camera calibration. *IEEE Transactions on Pattern Analysis and Machine Intelligence*, *22*(11), 1330–1334.

Zhou, J., Li, G., Wan, X., & Wang, J. (2016). A real-time computer vision-based platform for fabric inspection part 2: Platform design and real-time implementation. *The Journal of The Textile Institute*, *107*(2), 264–272.